

## Electronic Supplementary Information

# Fabrication of magnetic bimetallic $\text{Fe}_3\text{O}_4@\text{Au-Pd}$ hybrid nanoparticles with recyclable and efficient catalytic properties

Qingdong Xia, Shanshan Fu, Guojuan Ren, Fang Chai, \* Jingjie Jiang \* and Fengyu Qu \*

*Key Laboratory of Design and Synthesis of Functional Materials and Green Catalysis, Colleges of Heilongjiang Province, College of Chemistry and Chemical Engineering, Harbin Normal University, Harbin 150025, P. R. China. E-mail: fangchai@gmail.com, jiangjingjie80@163.com, qufengyuchem@hrbnu.edu.cn*

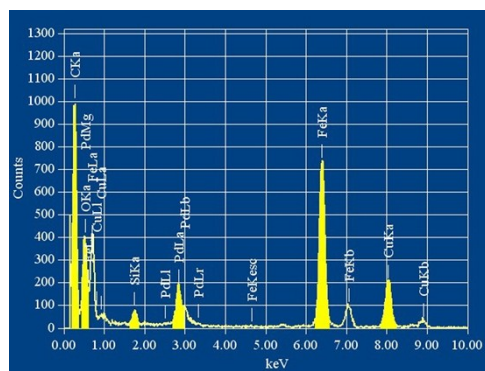


Fig. S1 EDS spectrum analysis of  $\text{Fe}_3\text{O}_4@\text{Pd}$  NPs.

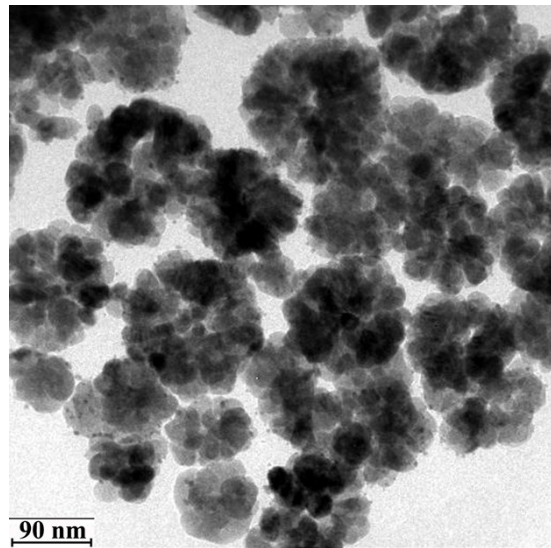


Fig. S2 TEM images of  $\text{Fe}_3\text{O}_4@\text{Au}$  nanoseeds.

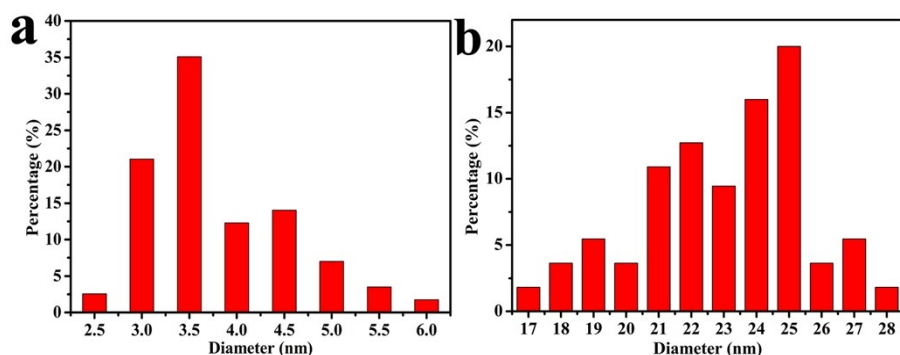


Fig. S3 The size distribution of Au NPs of (a)  $\text{Fe}_3\text{O}_4@\text{Au}$  nanoseeds and (b) Au-Pd NPs of  $\text{Fe}_3\text{O}_4@\text{Au-Pd}$  NPs.

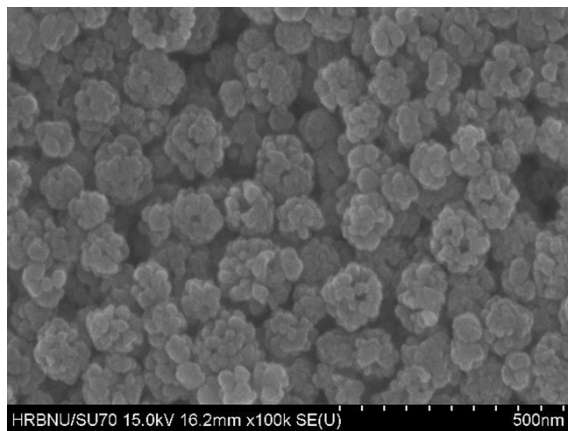


Fig. S4 SEM images of  $\text{Fe}_3\text{O}_4$  hollow spheres.

Specific surface areas of the samples were determined using N<sub>2</sub> adsorption–desorption isotherms at 77 k (Micromeritics TriStar II 3020) with the Brunauer–Emmett–Teller (BET) method. Fig. S5 shows the nitrogen adsorption desorption isotherms.

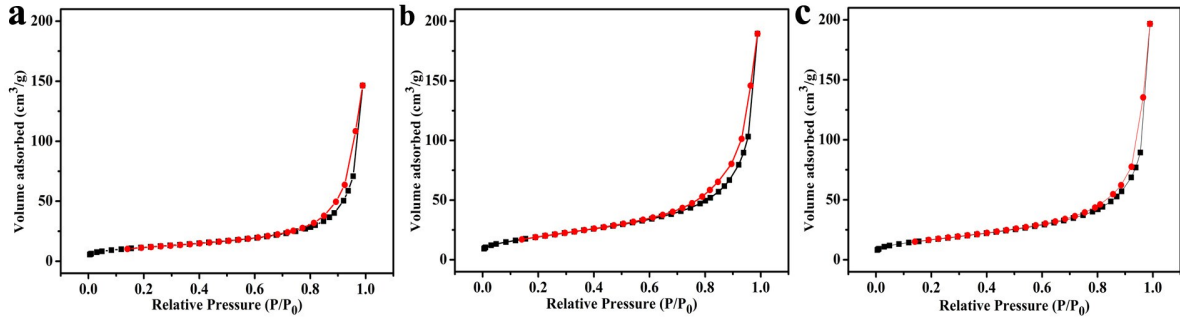


Fig. S5 N<sub>2</sub> adsorption/desorption isotherm of (a) Fe<sub>3</sub>O<sub>4</sub> hollow spheres, (b) Fe<sub>3</sub>O<sub>4</sub>@Pd NPs, (c) Fe<sub>3</sub>O<sub>4</sub>@Au-Pd NPs.

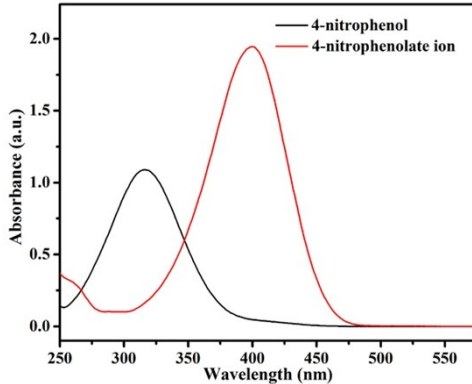


Fig. S6 The UV-vis characteristic peaks of freshly prepared 4-nitrophenol and 4-nitrophenolate ion aqueous solution at 317 and 400 nm, respectively.

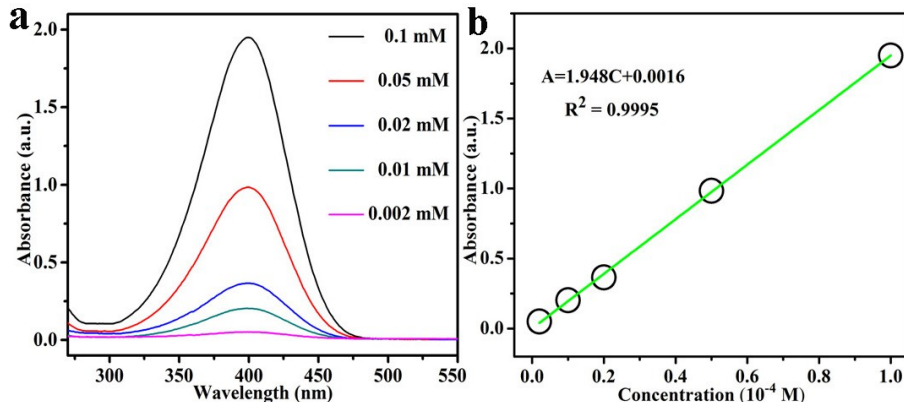


Fig. S7 (a) Absorption spectra of aqueous mixture solutions of 4-NP and NaBH<sub>4</sub> at different concentrations of 4-NP. (b) Plot of the peak absorbance against the concentration of 4-NP.

**Table S1** Rates of reaction and turnover frequencies (TOF)<sup>a</sup> for the reduction of 4-NP by catalyst.

<sup>a</sup> The TOF is defined as the moles of reduced 4-NP molecules per mole of the surface noble metal atoms per second.

Catalyst	Type	Rate constant (s <sup>-1</sup> )	TOF <sup>a</sup> (s <sup>-1</sup> )	References
Fe <sub>3</sub> O <sub>4</sub> @Au-Pd NPs	Supported	28.90 × 10 <sup>-3</sup>	8.78 × 10 <sup>-2</sup>	This work
Fe <sub>3</sub> O <sub>4</sub> @Pd NPs	Supported	14.50 × 10 <sup>-3</sup>	3.28 × 10 <sup>-2</sup>	This work
Au-Pd carbon spheres	Nanocomposites	14.60 × 10 <sup>-3</sup>	3.37 × 10 <sup>-3</sup>	1
Fe <sub>x</sub> O <sub>y</sub> /Pd@mSiO <sub>2</sub>	yolk-shell	1.60 × 10 <sup>-3</sup>	2.19 × 10 <sup>-3</sup>	2
Pd/Fe <sub>3</sub> O <sub>4</sub> /polypyrrol	hollow capsules	2.03 × 10 <sup>-3</sup>	1.47 × 10 <sup>-2</sup>	3
Pd@Au CSNTPs	core-shell	2.31 × 10 <sup>-3</sup>	2.46 × 10 <sup>-2</sup>	4
PdAu/Fe <sub>3</sub> O <sub>4</sub>	nanocomposites	5.47 × 10 <sup>-3</sup>	4.91 × 10 <sup>-2</sup>	5
Fe <sub>3</sub> O <sub>4</sub> @SiO <sub>2</sub> @CeO <sub>2</sub> @Au-Pd	nanocomposites	4.0 × 10 <sup>-3</sup>	5.69 × 10 <sup>-2</sup>	6

## References:

1. S. C. Tang, S. Vongehr, G. R. He, L. Chen and X. K. Meng, *J. Colloid. Interf. Sci.*, 2012, **375**, 125–133.
2. T. J. Yao, T. Y. Cui, X. Fang, F. Cui and J. Wu, *Nanoscale*, 2013, **5**, 5896–5904.
3. T. J. Yao, Q. Zuo, H. Wang, J. Wu, B. F. Xin, F. Cui and T. Y. Cui, *J. Colloid. Interf. Sci.*, 2015, **450** 366–373.
- 4 R. P. Zhao, M. X. Gong, H. M. Zhu, Y. Chen, Y. W. Tang and T. H. Lu, *Nanoscale*, 2014, **6**, 9273–9278.
- 5 Y. Tuo, G. F. Liu, B. Dong, J. T. Zhou, A. J. Wang, J. Wang, R. F. Jin, H. Lv, Z. Dou and W. Y. Huang, *Sci. Rep.-UK*, DOI: 10.1038/srep13515.
- 6 Q. Wang, W. J. Jia, B. C. Liu, A. Dong, X. Gong, C. Y. Li, P. Jing, Y. J. Li, G. R. Xu and J. Zhang, *J. Mater. Chem. A.*, 2013, **1**, 12732–12741.

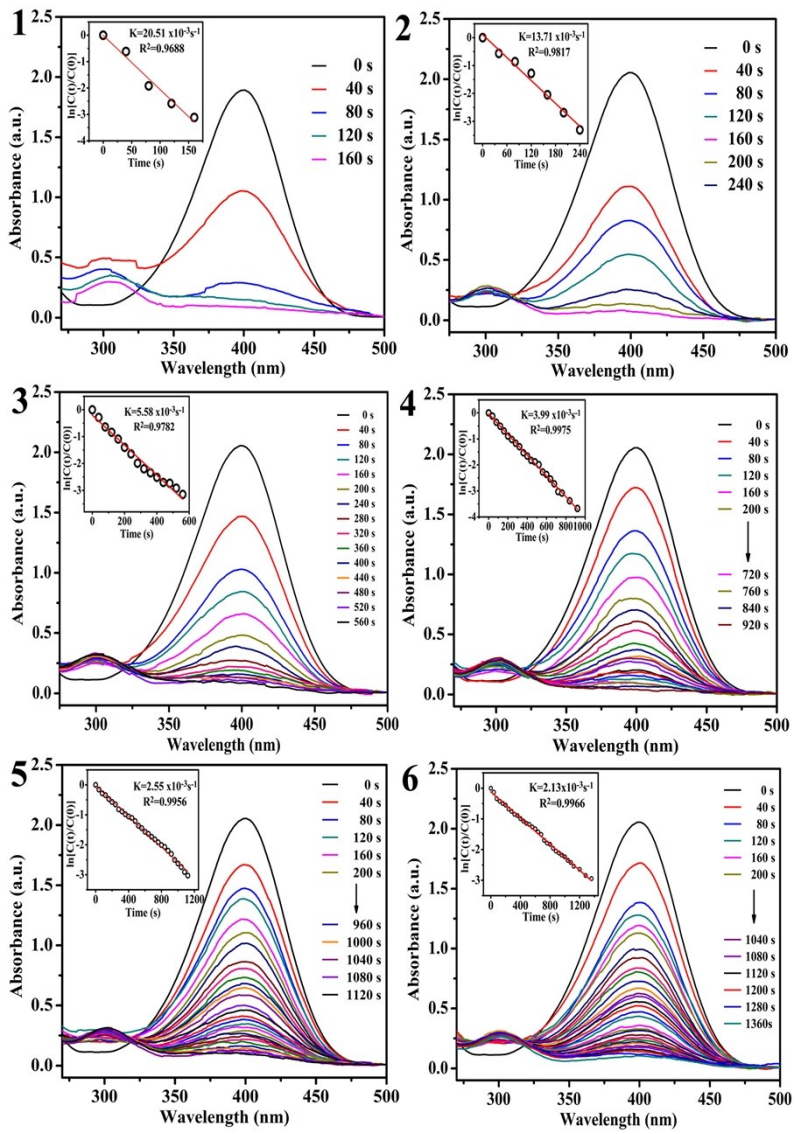


Fig. S8 The UV-vis spectra and kinetic rate of reduction of 4-NP by  $\text{NaBH}_4$  under the catalysis of  $\text{Fe}_3\text{O}_4@\text{Pd}$  NPs for 1-6 times.

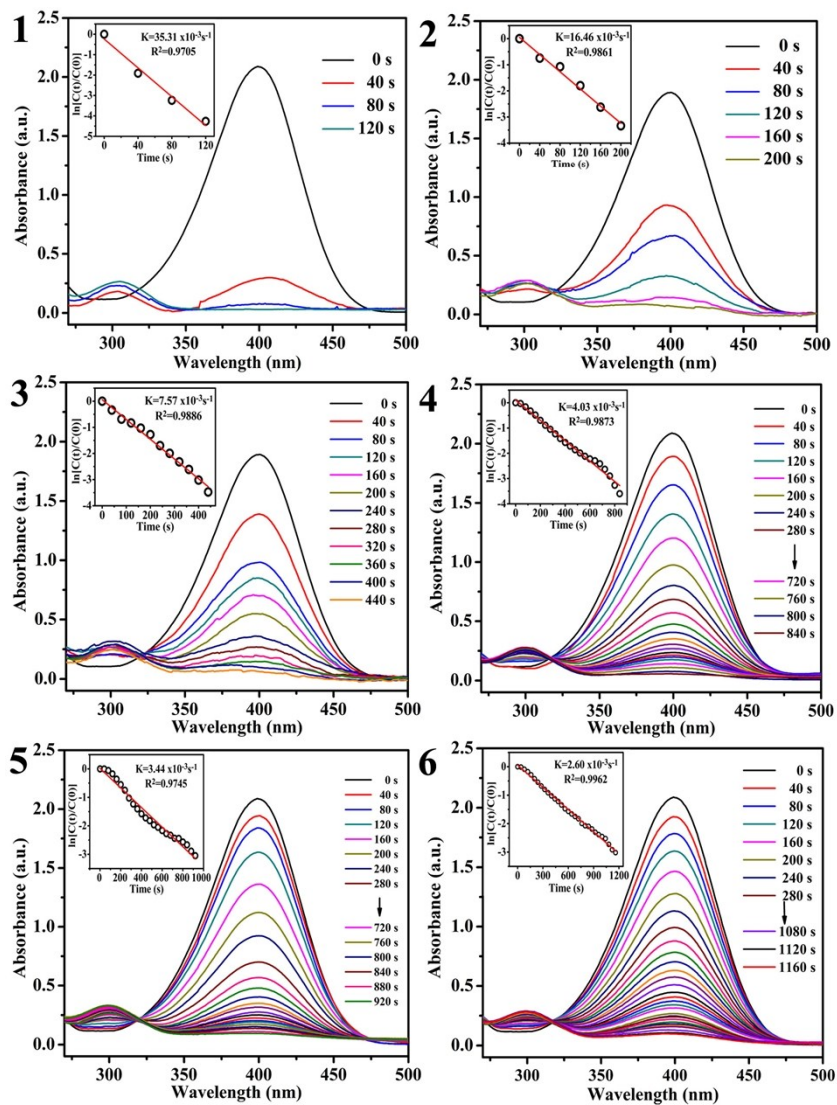


Fig. S9 The UV-vis spectra and kinetic rate of reduction of 4-NP by  $\text{NaBH}_4$  under the catalysis of  $\text{Fe}_3\text{O}_4@\text{Au-Pd}$  NPs for 1-6 times.

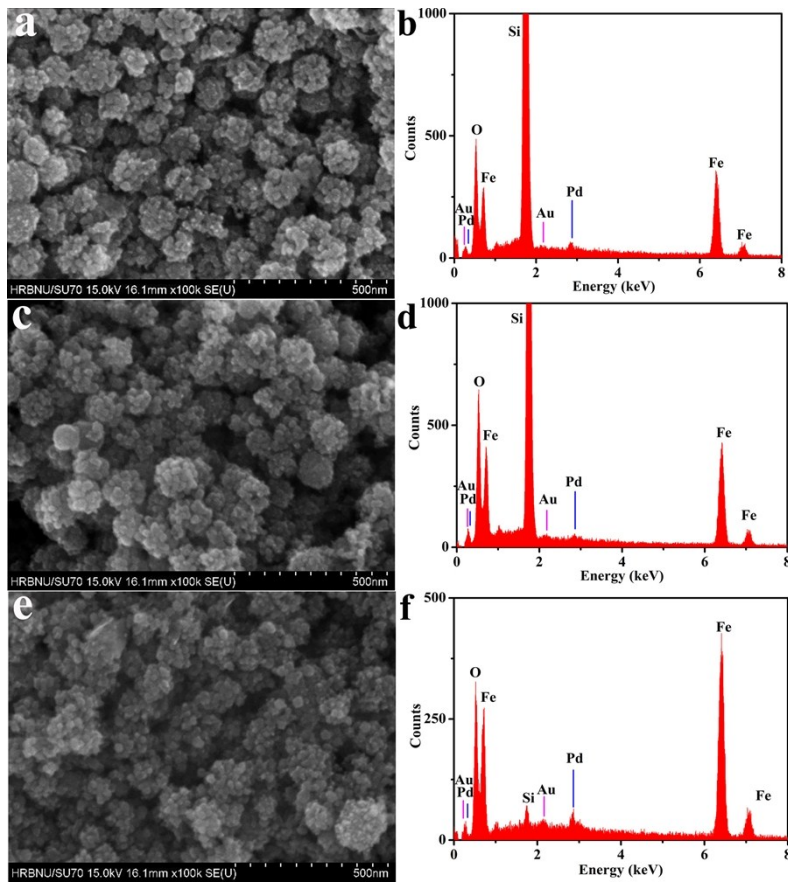


Fig. S10 The SEM (a, c, e) and EDX (b, d, f) of the  $\text{Fe}_3\text{O}_4@\text{Au-Pd}$  NPs as catalyst after reused 1<sup>st</sup>, 3<sup>rd</sup>, 6<sup>th</sup> times, respectively.

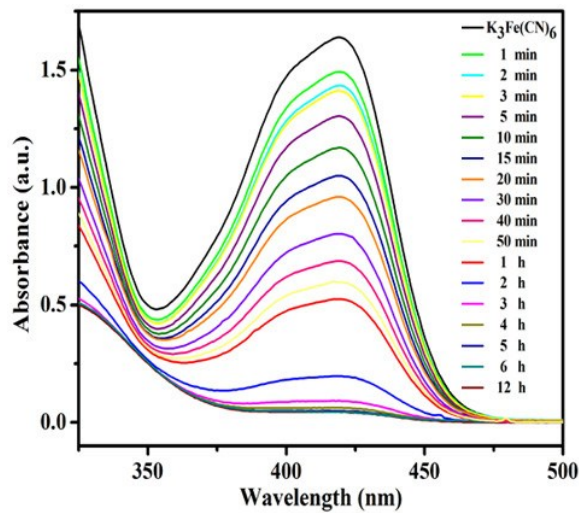


Fig. S11 UV-vis spectra of the reduction of  $\text{K}_3\text{Fe}(\text{CN})_6$  solution upon the addition of  $\text{NaBH}_4$  recorded at different times from 1 min to 12 h at 25°C,  $[\text{Fe}(\text{CN})_6]^{3-}=3\times 10^{-3}$  M,  $[\text{BH}^4]=0.04$  M in the absence of catalyst.

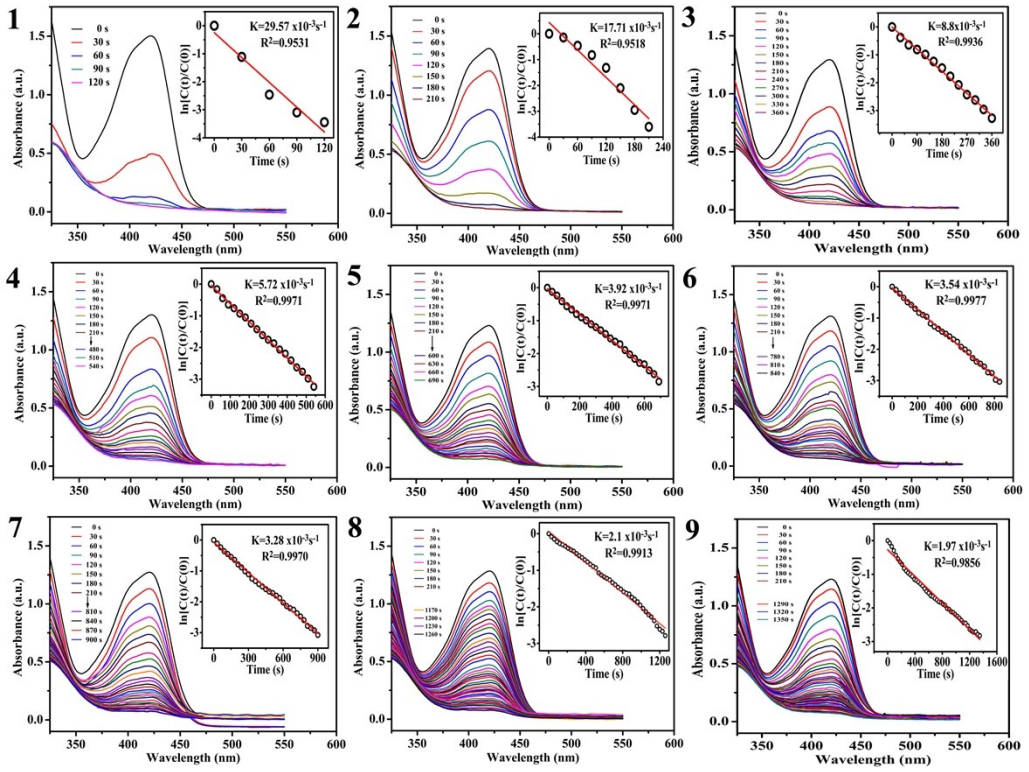


Fig. S12 The UV-vis spectra and kinetic rate of reduction of  $\text{K}_3\text{Fe}(\text{CN})_6$  by  $\text{NaBH}_4$  under the catalysis of  $\text{Fe}_3\text{O}_4@\text{Pd}$  NPs for 1-9 times.

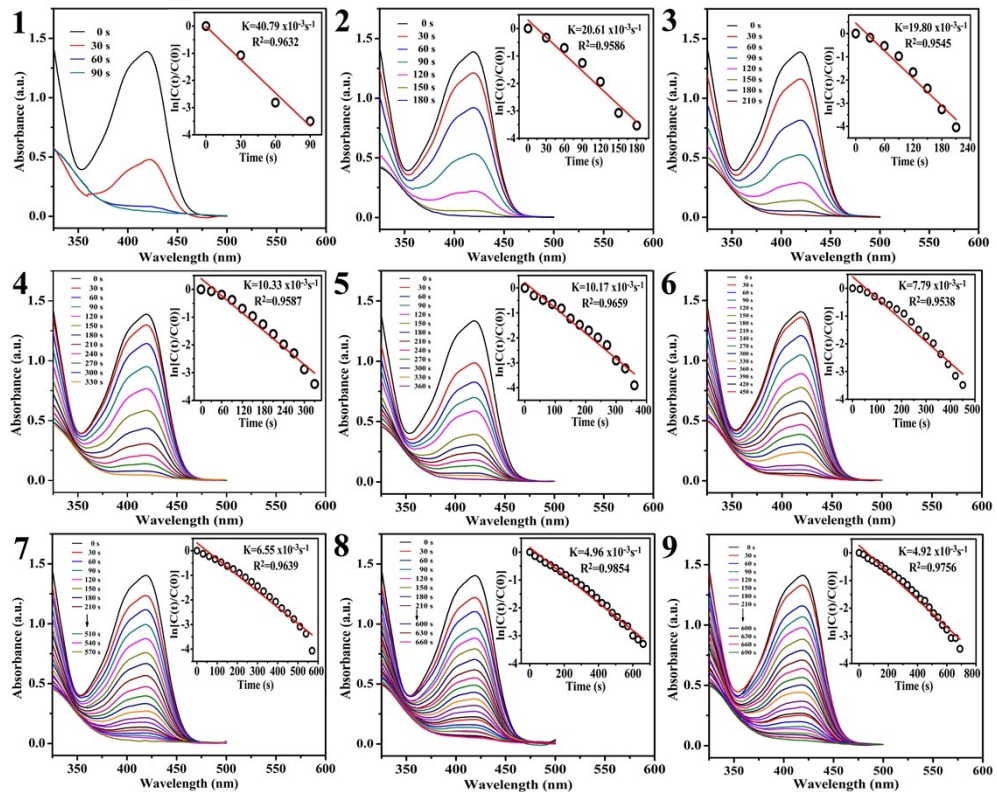


Fig. S13 The UV-vis spectra and kinetic rate of reduction of  $\text{K}_3\text{Fe}(\text{CN})_6$  by  $\text{NaBH}_4$  under the catalysis of  $\text{Fe}_3\text{O}_4@\text{Au-Pd}$  NPs for 1-9 times.

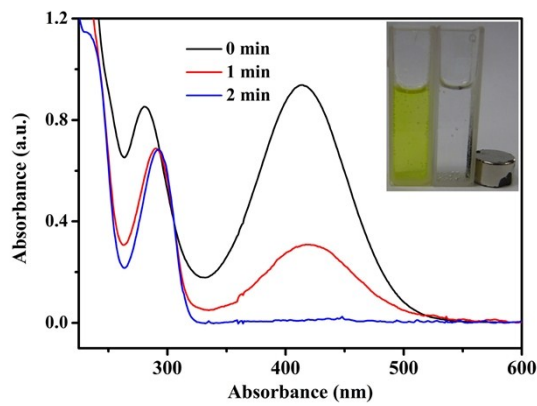


Fig. S14 UV-vis spectra of the reduction of 2-NP by NaBH<sub>4</sub> in the presence of Fe<sub>3</sub>O<sub>4</sub>@Au-Pd NPs,  
(2 mL H<sub>2</sub>O, 90 µL 10 mM 2-NP, 600 µL 0.5 M NaBH<sub>4</sub>).

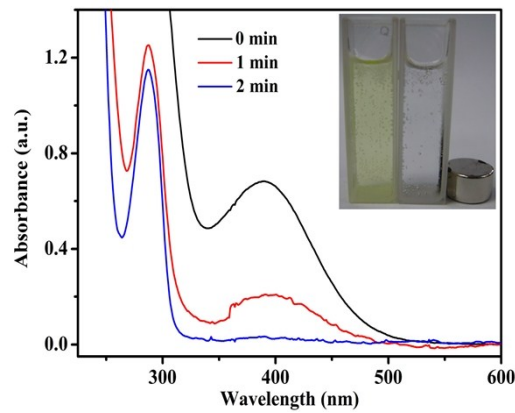


Fig. S15 UV-vis spectra of the reduction of 3-NP by NaBH<sub>4</sub> in the presence of Fe<sub>3</sub>O<sub>4</sub>@Au-Pd NPs,  
(2 mL H<sub>2</sub>O, 150 µL 10 mM 3-NP, 1 mL 0.5 M NaBH<sub>4</sub>).

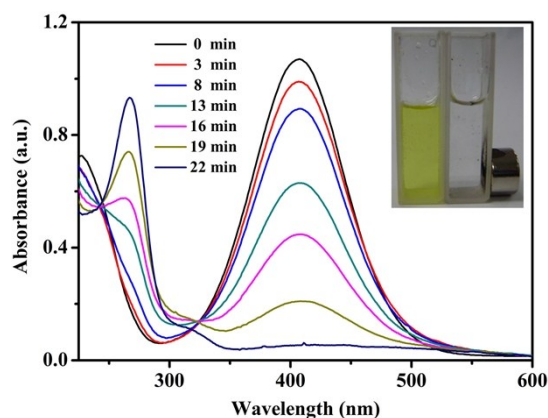


Fig. S16 UV-vis spectra of the reduction of 4-NTP by NaBH<sub>4</sub> in the presence of Fe<sub>3</sub>O<sub>4</sub>@Au-Pd  
NPs, (2 mL H<sub>2</sub>O, 25 µL 10 mM 4-NTP, 200 µL 0.5 M NaBH<sub>4</sub>).